Structures 91 (2026) 112641

Contents lists available at ScienceDirect

Structures

journal homepage: www.elsevier.com/locate/structures

Dynamic behaviour and serviceability performance of long-span CLT band-beam floor systems: Full-scale experimental study

Adam Faircloth [a,b,*], Hassan Karampour [a], Benoit P. Gilbert [a], Ian Underhill [a], Chandan Kumar [b]

[a] School of Engineering and Built Environment, Griffith University, Queensland, Australia
[b] Queensland Department of Primary Industries, Salisbury Research Facility, Brisbane, Australia

ARTICLE INFO

Keywords:
Floor vibration serviceability
Sustainable construction materials
Novel construction systems
Walking-induced vibration
Mass timber design

ABSTRACT

For the numerous characteristics that make cross-laminated timber (CLT) attractive to designers, such as its low density and high strength-to-weight ratio, they also contribute to increased sensitivity to low-frequency vibrations. CLT band-beams (BBs) offer a potential solution by reducing floor thicknesses, minimising supporting beam depths, and enabling longer spans (>8 m). This study experimentally investigates the dynamic behaviour and vibration serviceability of long-span CLT BB floor systems using a 9 m × 9 m laboratory floor comprising two CLT panel thicknesses and up to four BBs. The influence of BB span, CLT span, CLT thickness, screw connection density and inclination, and asymmetric superimposed dead load was investigated. Experimental modal analysis and controlled walking tests (1.4–2.1 Hz) were used to evaluate modal properties and vibration response in terms of weighted acceleration and vibration dose value (VDV). BB span was found to govern both modal behaviour and walking-induced response, whereas CLT span had a secondary influence. Increasing connection density enhanced stiffness but reduced damping, while screw inclination had only a minor effect. The inclusion of resilient material increased Mode 1 damping by approximately 30–35%. All measured VDVs remained below 0.22 $m \cdot s^{-1.75}$, indicating a low probability of adverse comments and demonstrating the suitability of CLT BB floors for long-span applications.

1. Introduction

As the use of mass timber grows, so too do the amount of novel design solutions, aimed at either achieving open floor plans through longer spans, reduced need for concrete additions or 'wet trades' as a serviceability topping, and reducing supporting beam depths to increase ceiling heights [1–8]. However, with each of these modifications, serviceability becomes specifically sensitive and therefore needs to be understood. Increasing the span of floor systems consequently reduces the floors natural frequency, making it more sensitive to induced vibrations [9–11]. This phenomenon is not isolated to timber floor systems, as such other building materials are governed by the same design constraints and corresponding influences they will have on perceived performance and vibrational serviceability [12,13].

Reduced floor thickness can also contribute to higher accelerations resulting from footfall induced vibrations requiring a damping solution where often concrete is selected or larger supporting beams are required [14]. To address these challenges in span sensitivity and supporting beam depth, one potential system being developed is the CLT band-beam (BB). A CLT BB takes advantage of the 2-way spanning action potential of CLT, often with a larger width compared to a glulam beam, therefore reducing torsional displacements and effectively reduce beam depth [15,16]. The use of BBs in practice has been sparing with few structures using them such as Limberlost Place in Toronto Canada [17] and the Maryborough Fire Station (MFS) in Maryborough Australia [18], with several studies also highlighting its potential. Gleason [19] evaluated two theoretical mass timber floor systems as a conventional post-and-plate design using CLT and glulam columns, and a BB supported CLT floor with glulam columns for their critical bending moments. The column grid spacing in both systems was 3.0 m (BB span) × 3.6 m (CLT span) with a 175 mm thick 5-layer CLT floor. The 5-layer band-beams were 1200 mm wide and 175 mm thick. The results of the study highlighted the BBs were being relied on for a significant portion of the bending moments associated with the floor, exceeding the allowable limits of 5.6 kN·m/m as specified in the CLT Handbook developed by FPInnovations [20]. However, inconsistencies in fixity modelling and span sensitivity remain unanswered as to potential

* Corresponding author at: School of Engineering and Built Environment, Griffith University, Queensland, Australia.
E-mail address: Adam.Faircloth@dpi.qld.gov.au (A. Faircloth).

https://doi.org/10.1016/j.istruc.2026.112641
Received 17 March 2026; Received in revised form 25 June 2026; Accepted 13 July 2026
Available online 17 July 2026

Nomenclature

BB	Band-beam.
CLT	Cross-laminated timber.
CL3, CL5	Three- and five-layer CLT panels.
TF	Test floor configuration.
CT	Connection type.
SDL	Superimposed dead load (kg/m^2).
EMA	Experimental modal analysis.
FRF	Frequency response function.
MMC	Modal mass contribution (%).
CoV	Coefficient of variation.
f	Natural frequency (Hz).
f_w	Walking frequency (Hz).
ζ	Damping ratio (%).
$a_w(t)$	Frequency-weighted vertical acceleration response (m/s^2).
$a_{w\text{-}RMS\text{-}max}$	Maximum frequency-weighted RMS acceleration over a 1 s interval (m/s^2).
VDV	Vibration dose value over the duration of the vibration event (m·s$^{-1.75}$).
T	Signal duration (s).
W_k	Frequency weighting function.
E_{Major}	Effective major-axis modulus of elasticity (MPa).
E_{Minor}	Effective minor-axis modulus of elasticity (MPa).
G	Effective shear modulus (MPa).
L_B	Band-beam span (m).
L_{F1},L_{F2}	CLT panel spans (m).
e_l	Clear spacing between adjacent internal band-beam supports (m).
d	Screw diameter (mm).
a_1	Longitudinal screw spacing (mm).
a_2	Transverse screw spacing (mm).
e	Screw edge distance (mm).
θ	Screw inclination angle (°).
l_{ef}	Effective screw embedment length (mm).

remediation methods which would contribute to more realistic moment capacities.

Guo et al. [16] investigated the vibrational performance of a BB supported timber concrete composite (TCC) floor system in both a laboratory and in-situ (Limberlost place, Toronto Canada) environment. The laboratory test was performed on a 7-layer CLT panel (245 mm) over a 9.2 m span length of the BB TCC floor with a width of 2.4 m. The in-situ floor had a CLT thickness of 244 mm with a grid spacing of 9.2 m (BB span) and 4.8 m (CLT span). The laboratory analyses highlighted natural frequencies ranging from 7.5 to 7.9 Hz where the small variations were due to changes in fixity and other such connection methods. In-situ analysis also highlighted a 18.7% difference in the measured frequency of the two approaches with in-situ testing detecting a 6.1 Hz first modal frequency. This difference also extended to the acceleration measurements with unacceptable values being received in the laboratory but acceptable measurements in-situ (0.003 m/s^2). These differences are hypothesised to be a result of the accuracy of the setup, specifically the lack of two-way spanning configuration in the laboratory environment while the building did consist of such a setup [21].

Based on the existing limited literature, the vibrational serviceability of CLT BB floor systems is relatively unexplored and underdefined. Aspects such as span sensitivity, connection density, and loading scenarios are identified gaps that this study aims to investigate under walking-induced excitations. To achieve this, laboratory testing was conducted on BB-supported CLT floors with a maximum footprint of 9 m by 9 m, which allows for the evaluation of different configurations and loading conditions. Experimental modal analysis (EMA) and footfall-induced vibration tests were performed to assess the floors' natural frequencies, damping, modal mass, and vibration serviceability. The article structure begins with a description of the materials used through the experiments (Section 2.1), how they have been configured, i.e. floor system setup and testing (Section 2.2), and experimental methods (Section 2.3). The results and discussion outlined through Section 3 have been separated into span sensitivity and CLT thickness investigation (Sections 3.1 and 3.2), influence of fixities on modal and walking properties (Sections 3.3 and 3.4), and vibrational performance of floor system with distributed load (Sections 3.5 and 3.6). Finally, Section 4 summarises the main findings and presents the conclusions drawn from this study.

2. Materials, configurations and methods

2.1. Materials

Twelve (12) CLT panels, comprising six 3-layer (CL3, 120 mm thick) and six 5-layer (CL5, 220 mm thick) configurations, together with four (4) band beams (BBs) were supplied by XLam Australia for use in this study. All CLT panels and BBs were manufactured to a uniform length of 9 m. The cross-sectional configurations of the CLT panels and BB members are presented in Fig. 1. The CLT and BB elements were fabricated using sawn timber boards graded under XLam's proprietary XGP1 and XGP2 layup classifications [22]. These layups correspond to specific structural performance grades based on lamella strength and stiffness properties, where XGP1 typically represents higher structural grade outer laminations to maximise bending stiffness and strength, while XGP2 denotes structural-grade internal laminations. The CLT panels and BBs were assessed for their bending frequencies to then back-calculate the effective mechanical properties (elastic moduli). Following the analytical procedure described by Faircloth et al. [15], the dynamic elastic moduli (E_x, E_y, G_{xy}) was derived from the identified bending modes, accounting for the measured material density of each specimen. The analytical formulation is not repeated here for brevity. The resulting mechanical properties are summarised in Table 1.

Screw used in this study varied depending on floor thickness and inclination with nominal lengths of 100 mm (HBS8100), 180 mm (HBS8180), 200 mm (HBS8200), 300 mm (HBS8300), and 440 mm (HBS8440). In addition, approximately 250 linear metres of 75 mm wide Aladin soundproofing resilient material were provided by Rothoblaas Australia. The supplied resilient materials were installed over the surface of the BBs in contact with the CLT as well as in the lap joint between CLT panels. The testing which relates to the use of the Aladin is detailed in future sections of this article.

2.2. Methods

The following sections describe the testing methods for the data collection from modal and walking experiments and the floor configurations explored through this study.

2.2.1. Experimental Modal Analysis

Experimental modal analysis (EMA) was used to identify the dynamic properties of the CLT band-beams (BB) floor systems, including natural frequencies, damping ratios, modal masses, and mode shapes with the schematic of the various test setups shown in Fig. 2. A National

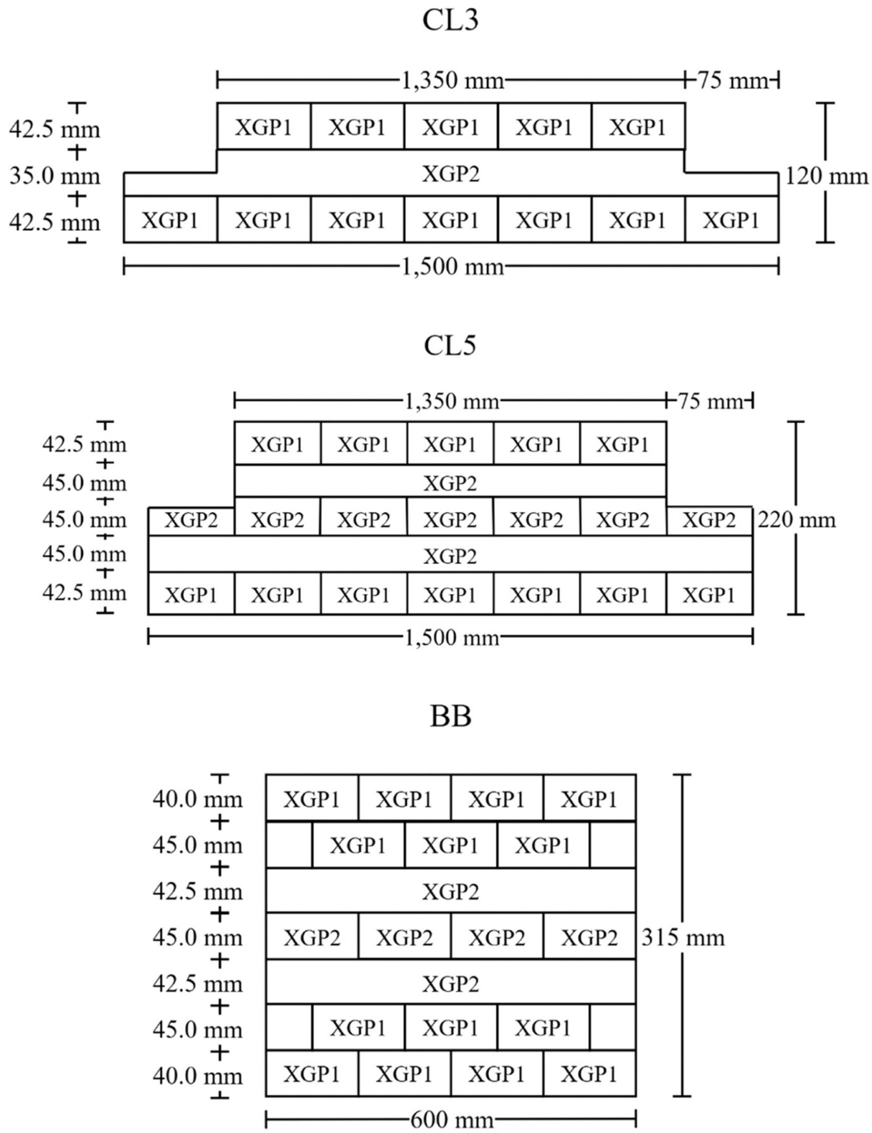

Fig. 1. Cross-sectional layouts of CL3 (120 mm), CL5 (220 mm), and band-beam (BB) members showing lamella thicknesses and XLam layup grades (XGP1 and XGP2) [18].

Table 1
Mechanical properties of the CLT panels and band-beams calculated from EMA results using the analytical method by Faircloth et al. [23].

Product	Density (kg/m^3)	E_{Major} (MPa)	E_{Minor} (MPa)	G (MPa)
CL3	481.5 (14.1)	9873 (15.0)*	1307 (3.02)	280.0 (7.17)
CL5	475.2 (12.0)	10,071 (9.87)	1114 (7.69)	301.1 (3.11)
BB	480.1 (7.54)	10,926 (11.3)	–	–

* CoV is given in the brackets.

Instruments sound and vibration module (NI 9234) was used to acquire acceleration and force data with LabVIEW (ver. 2017, National Instruments). For all EMA tests, the sampling rate and sample size were fixed at 10 kHz and 30,000 samples, respectively. The measured signals were passed through a 50 Hz low-pass filter prior to analysis to remove high-frequency noise components. For EMA of the test floors, a fixed-impact testing approach was adopted. Twelve surface-mounted single-axis accelerometers (A1–A12, sensitivity ≈100 mV/g) were distributed across the floor surface as shown in Fig. 2a. An impact hammer (IEPE, sensitivity 240 mV/N) was then used to excite the floor system.

For each floor configuration, multiple impact events were applied at a fixed excitation location and the corresponding frequency response functions (FRFs) were averaged prior to modal identification. To assess measurement consistency, the responses recorded by the 12 accelerometers for a representative floor configuration (TF1) are presented in Fig. 3. Although variations in response amplitude are observed between channels due to their different positions relative to the modal deflected shapes, the dominant resonance peaks occur consistently across the measurement grid. This indicates good repeatability of the measurements and confirms that the averaged FRFs used for modal parameter estimation are representative of the global floor behaviour.

Post-processing was performed using ARTeMIS Modal (version 8.0) for frequency, damping, modal mass and mode shapes for the first four modes on all tested BBs and floor systems. These modes were selected to ensure that the dynamic behaviour up to and beyond twice the first natural frequency was captured [24]. Fig. 3 presents the frequency response functions obtained from the 12 accelerometer channels for the representative TF1 floor configuration. Despite variations in response amplitude between measurement locations, the dominant resonance peaks are consistently identified across the floor, demonstrating good repeatability of the experimental measurements.

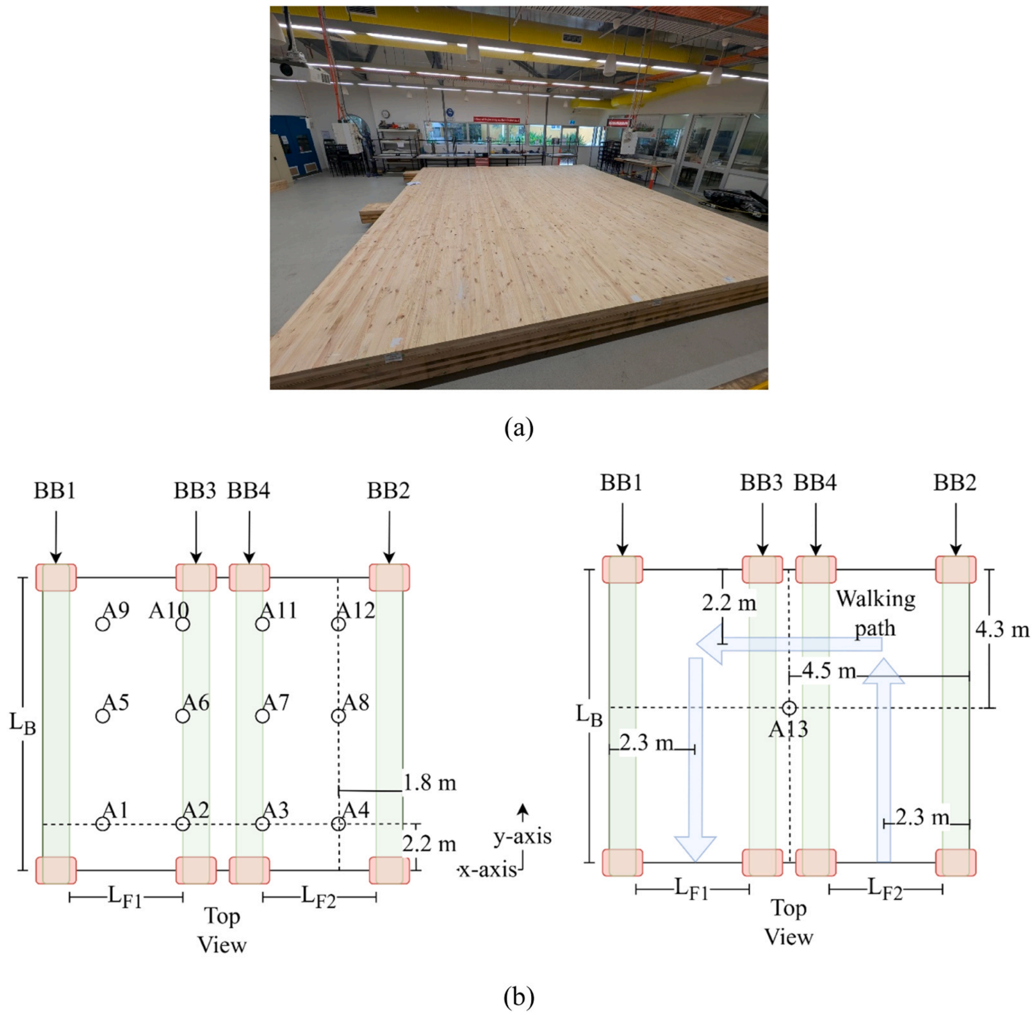

Fig. 2. (a) Images of CLT floor and BB EMA configuration, and (b) schematics showing EMA sensor and walking path experimental setup for CLT floor tests.

Given the two main methods available to calculate damping, temporal and logarithmic [25–28], it is important to note the method ARTeMIS Modal uses. As the purpose of this study has been to investigate the modal properties of each floor system, a logarithmic damping method has been considered most appropriate. ARTeMIS Modal uses the modal identification method where parameters are identified from a singular value extracted from the signals' FRF matrix, with damping ratios estimated from the identified resonance peaks [26]. Damping is extracted from fitting either a state space model (SSI) or a rational polynomial (EFDD, CMIF and RFPZ) [29]. When a rational polynomial is fitted then the roots of the denominator polynomial are determined and the natural frequency and damping ratio is extracted.

It is acknowledged that damping estimates are more sensitive to excitation level and signal quality than natural frequencies. Accordingly, the damping ratios reported in this study are interpreted as representative modal estimates rather than exact deterministic values. As an additional verification, a representative CLT floor configuration was tested using both impact hammer excitation and heel-drop excitation. For the first mode, the impact hammer EMA identified (f_1= 5.85 Hz) and (ζ_1 = 3.70%), while the heel-drop OMA identified (f_1 = 5.86 Hz) and (ζ_1 = 3.41%). The frequency difference was less than 1% and the damping difference was approximately 7.8%, indicating that the impact hammer method provided comparable Mode 1 damping estimates for the purpose of assessing relative trends between configurations.

2.2.2. *Foot-fall Induced Vibration*

Footfall-induced vibration tests were performed on each floor configuration at controlled walking frequencies of 1.4, 1.6, 1.8, and 2.1 Hz by a single test subject with a body mass of 80 kg, wearing steel toed footwear (boots) and maintaining a stride length of ~600 mm. The walking frequency range was selected in accordance with established design standards to capture typical human walking rates [30]. A surface-mounted accelerometer (A13) was installed at the location shown in Fig. 2b to capture maximum expected vertical response; the walking path is also indicated in the figure. Following completion of the experiments, the recorded acceleration data were post-processed using RStudio (version 4.4.1). In accordance with established vibration serviceability standards [31,32], floor performance was characterised using the maximum root mean square acceleration, $a_{w\text{-}rms\text{-}max}$, and the vibration dose value (VDV). The quantity $a_{w\text{-}rms\text{-}max}$, represents the highest root mean square acceleration obtained over a one-second interval and provides an indication of the peak vibration severity experienced by occupants. In contrast, the VDV is calculated over the duration of the vibration event and incorporates both vibration magnitude and exposure time through a fourth-power relationship, making it particularly sensitive to transient and intermittent excitations such as walking-induced vibrations. Lower values of both metrics correspond to improved vibration performance and enhanced occupant comfort.

$$a_{w-rms} = \sqrt{\frac{1}{T}\int_0^T a_w(t)^2 dt} \tag{1}$$

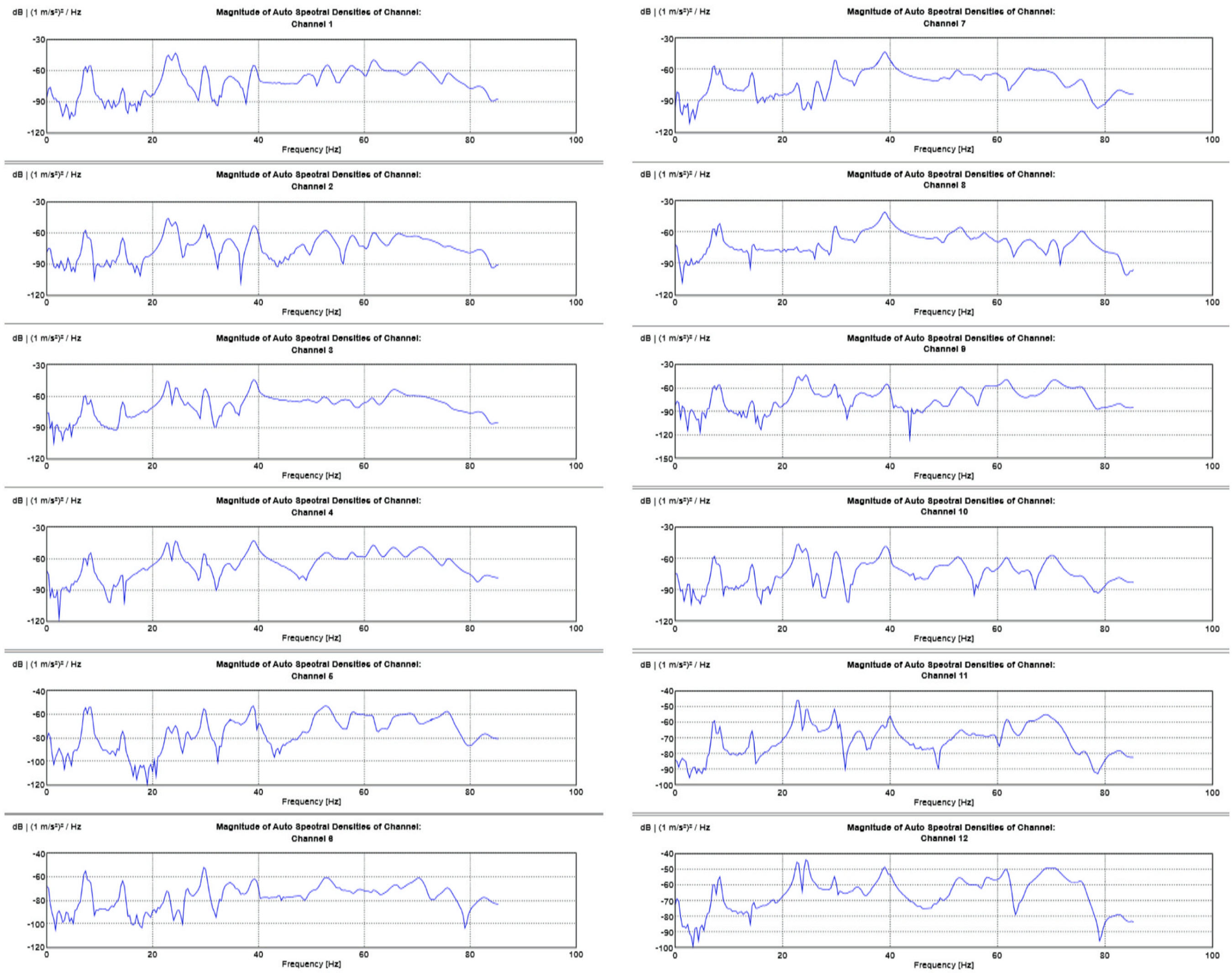

Fig. 3. Frequency response function plots from 12 accelerometers showing the dominant frequencies from a full grid of testing over a test floor setup for TF1 as detailed in Table 2.

$$VDV = \left[\int_0^T a_w^4(t)dt \right]^{1/4} \quad (2)$$

.

The maximum RMS acceleration provides a measure of the peak vibration intensity, whereas the VDV reflects the cumulative effect of

Table 2
Geometric parameters and configuration details of the investigated CLT band-beam floor systems. The floor layouts defining these parameters are shown in Fig. 2.

Test Foor	L_{F1} (m)	L_{F2} (m)	e_l (m)	CLT	BB1	BB2	BB3	BB4	L_B (m)	Resilient Material
TF1	2.5	2.5	0.3	CL5	✓	✓	✓	✓	9.0	✓
TF2	4.2	4.2	0.0	CL5	✓	✓	✓	✓	9.0	✓
TF3	7.8	–	–	CL5	✓	✓	–	–	9.0	✓
TF4	7.8	–	–	CL5	✓	✓	–	–	8.0	✓
TF5	7.8	–	–	CL5	✓	✓	–	–	7.0	✓
TF6	7.8	–	–	CL5	✓	✓	–	–	6.0	✓
TF7	7.8	–	–	CL5	✓	✓	–	–	5.0	✓
TF8	6.6	–	–	CL5	✓	✓	–	–	9.0	✓
TF9	6.6	–	–	CL5	✓	✓	–	–	8.0	✓
TF10	6.6	–	–	CL5	✓	✓	–	–	7.0	✓
TF11	6.6	–	–	CL5	✓	✓	–	–	6.0	✓
TF12	6.6	–	–	CL5	✓	✓	–	–	5.0	✓
TF13	7.8	–	–	CL3	✓	✓	–	–	9.0	✓
TF14	7.8	–	–	CL3	✓	✓	✓	–	7.8	✓
TF15	6.9	0.9	–	CL3	✓	✓	✓	–	9.0	✓
TF16	5.4	1.4	–	CL3	✓	✓	✓	–	9.0	✓
TF17	2.5	2.5	0.3	CL3	✓	✓	✓	✓	9.0	✓
TF18	4.2	4.2	0.0	CL3	✓	✓	✓	✓	9.0	✓

vibration exposure and is particularly suitable for assessing transient walking-induced floor vibrations. These response quantities may be compared against serviceability criteria specified in relevant standards to evaluate occupant comfort.

2.3. Floor configurations

The following section describes the various exploration phases of the project such as span sensitivity, fixities, and superimposed load (SDL).

2.3.1. Influence of span and CLT thickness

The floor configurations investigated in this study are summarised in Table 2 with all being tested under simply-supported boundary conditions; clear spans for BBs achieved by contact supports). Each configuration comprised a one-way CLT panel system with a total surface area dimension of 9 m × 9 m, supported by two to four band beams (BBs) as described in Table 2. By varying the number of BBs from two to four, different CLT spans were achieved, allowing evaluation of span sensitivity.

2.3.2. Influence of fixities

The influence of fastener spacing and inclination on the composite behaviour of the CLT BB floor system was investigated, as shown in Fig. 4 and summarised in Table 3. To evaluate the influence of screw spacing, a staged reduction in fastener spacing was implemented at the CLT–BB interfaces and at the lapped CLT panel joints (as shown in Fig. 4). As part of this fixity investigation, the change in performance seen through the use of the Aladin resilient soundproofing material has been investigated as detailed in Table 3 between CT6 (without Aladin) and CT7 (with Aladin). It was hypothesised that the Aladin resilient soundproofing material would yield an increase in measured damping ratios [28,33]. To further examine the degree of composite action achievable within the system, two screw inclination angles (90° and 45°) were investigated (see Fig. 4g). The inclined configuration was intended to enhance mechanical interlock between the CLT and BB elements. To maintain comparable embedment depths for both vertical (90°) and inclined (45°) screws, the screw lengths were adjusted according to the CLT thickness (CL3 or CL5).

2.3.3. Influence of superimposed load

Superimposed load tests were conducted to investigate the influence of additional distributed mass on the vibrational serviceability of the TF1 and TF17 floor configurations. A nominal superimposed load (SDL) of ~30 kg/m^2 was applied using water bladders asymmetrically to one side of the floor surface, representing a non-uniform loading condition typical of partition walls or localised occupancy loads (Fig. 5). The bladders were arranged to simulate a uniformly distributed load across the floor surface. The water bladders were filled incrementally, and deflection readings were recorded at intervals of approximately 10 kg/m^2 (corresponding to ~315 L per fill). All SDL floor assessment include the use of the Aladin resilient soundproofing material.

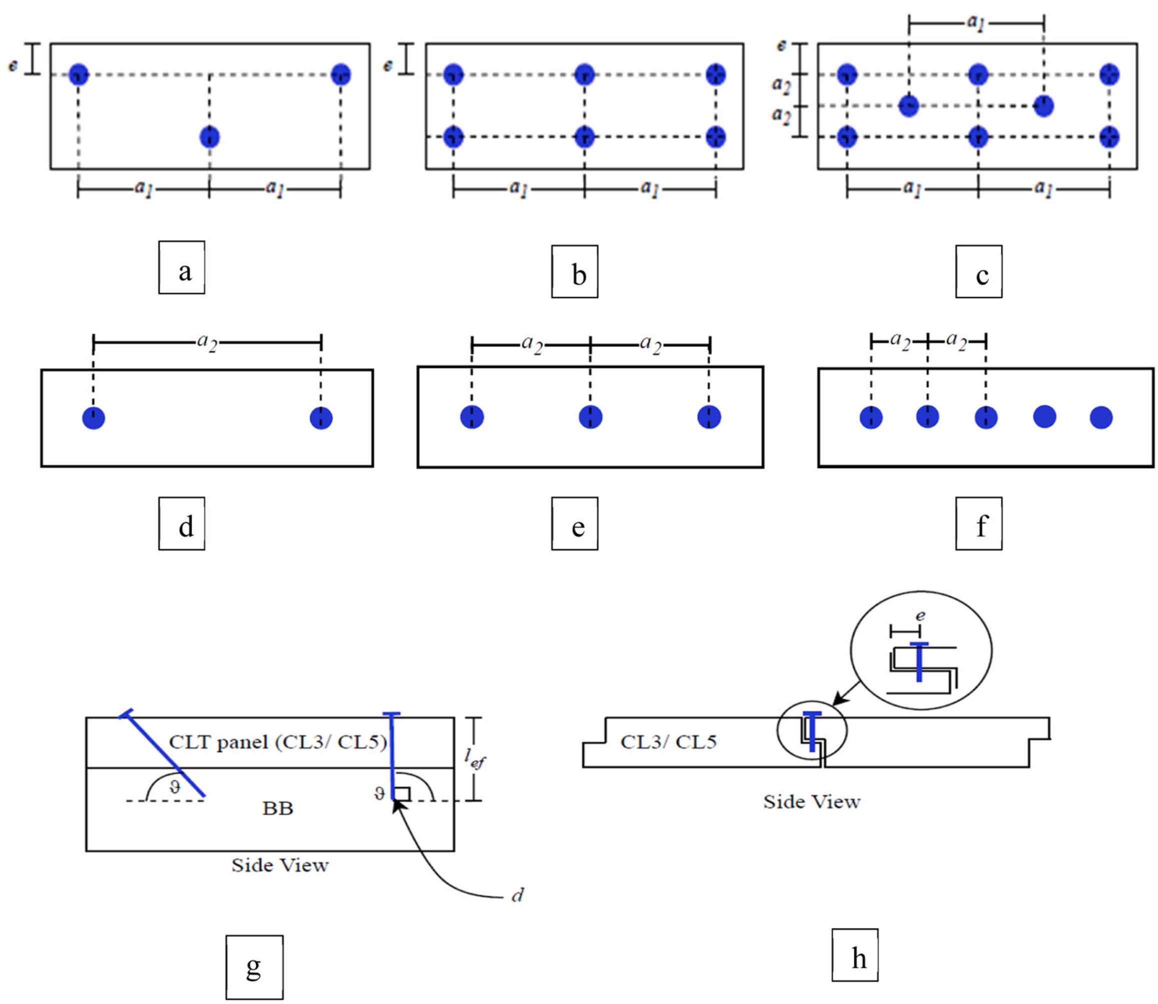

Fig. 4. Screw spacing and inclination configurations investigated, including plan views (a–f) and cross-sectional installation details (g–h). Geometric parameters are defined in Table 2.

Table 3
Geometric parameters and configuration details of the investigated CLT band-beam floor systems. The plan and cross-sectional layouts defining these parameters are shown in Fig. 3.

Connection Type	Member 1	Member 2	Resilient Material	*d* (mm)	a_1 (mm)	a_2 (mm)	*e* (mm)	ϑ (°)	l_{ef} (mm)	Figure 4	Floor type***
CT1	CL3	BB	–	8	500	–	32.5	90	200	4a	TF18
CT2	CL3	BB	–	8	500	–	32.5	90	200	4b	TF18
CT3	CL3	BB	–	8	500	–	32.5	90	200	4c	TF18
CT4	CL3	CL3	–	8	500	1000	32.5	90	100	4c + 4d	TF18
CT5	CL3	CL3	–	8	500	500	32.5	90	100	4c + 4e	TF18
CT6	CL3	CL3	–	8	500	250	32.5	90	100	4c + 4 f	all
CT7	CL3	BB	✓	8	500	250	32.5	90	100	4c + 4 f	all
CT8	CL3	BB	✓	8	500	250	32.5	45*	440	4 g	TF17
CT9	CL3	BB	✓	8	500	250	32.5	45**	440	4 g	TF17
CT10	CL5	BB	✓	8	500	250	32.5	90	300	4c + 4 f	all
CT11	CL5	BB	✓	8	500	250	32.5	45*	440	4 g	TF1
CT12	CL5	BB	✓	8	500	250	32.5	45**	440	4 g	TF1

* Half of BB−3 screws are removed and inserted at 45° angle to the CLT face.
** All BB−3 screws are removed and inserted at 45° angle to the CLT face.
*** See Table 1.

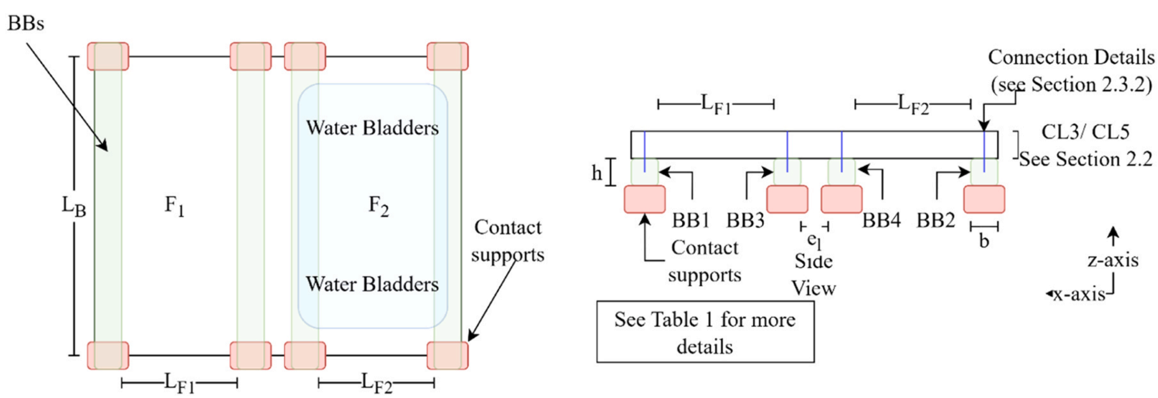

Fig. 5. Floor configurations showing plan and cross-sectional views. The CLT panels are oriented along the *x*-axis, while the band beams (BBs) span in the *y*-axis direction.

3. Results and discussion

3.1. Influence of span and CLT thickness on modal properties

The identified modal properties for the floor configurations introduced in Table 2 are summarised in Table 4, with representative mode shapes then shown in Fig. 6. The reported mode shapes are only for those floor systems without and with BB(s) in the centre of the floor. The first four modes for each configuration were extracted to capture the dominant global bending behaviour of each floor system. The modal shapes illustrate clear two-way bending action, with the fundamental mode dominated by global flexure of the CLT panels supported by the band beams, and higher modes exhibiting increased nodal lines in both principal directions. A comparison between the CL3 and CL5

Table 4
Experimental modal properties of floor configurations with varying CLT thickness and span parameters.

Test Floor	Connection Type	Mode 1			Mode 2			Mode 3			Mode 4		
		f (Hz)	ζ (%)	MMC (%)	*f* (Hz)	ζ (%)	MMC (%)	*f* (Hz)	ζ (%)	MMC (%)	*f* (Hz)	ζ (%)	MMC (%)
TF1	CT9/ CT6	8.83	3.24	67.1	14.3	1.46	31.5	24.4	0.44	0.81	29.7	0.27	0.64
TF2	CT9/ CT6	8.03	3.00	79.8	13.1	2.01	19.0	22.0	1.01	0.89	30.1	0.99	0.28
TF3	CT9/ CT6	3.51	3.00	81.3	7.00	5.27	16.3	12.5	3.58	1.90	16.4	1.04	0.49
TF4	CT9/ CT6	4.37	3.36	72.5	7.80	1.13	24.2	13.5	1.99	2.64	18.9	0.93	0.68
TF5	CT9/ CT6	4.81	4.04	78.3	8.25	3.83	18.3	16.1	2.23	3.21	21.8	1.67	0.21
TF6	CT9/ CT6	5.87	4.34	80.0	8.83	1.96	18.9	18.5	1.89	0.84	24.3	0.73	0.28
TF7	CT9/ CT6	6.39	4.78	75.0	8.98	3.04	23.7	21.1	3.05	0.96	25.2	2.66	0.32
TF8	CT9/ CT6	5.67	3.24	90.8	11.2	2.87	6.76	15.7	2.21	1.94	22.7	1.52	0.54
TF9	CT9/ CT6	6.29	3.70	87.9	11.2	2.45	8.93	15.2	2.24	2.13	21.7	2.24	1.04
TF10	CT9/ CT6	6.75	4.35	74.4	11.8	3.83	23.8	16.4	1.16	1.44	26.0	2.51	0.36
TF11	CT9/ CT6	7.44	4.72	83.9	11.9	2.86	13.5	18.1	2.76	2.47	26.7	2.26	0.19
TF12	CT9/ CT6	7.76	5.46	79.5	12.0	2.78	16.9	19.9	2.42	3.43	27.1	2.79	0.21
TF13	CT3/ CT6	3.33	1.09	97.5	5.56	2.26	1.93	7.31	2.84	0.23	16.6	0.67	0.34
TF14	CT3/ CT6	6.00	1.75	92.7	10.5	1.49	5.51	12.5	2.01	0.63	17.5	0.98	1.11
TF15	CT3/ CT6	4.00	0.95	91.6	6.50	3.51	6.26	10.2	5.36	0.86	30.2	0.69	1.24
TF16	CT3/ CT6	5.00	2.12	86.6	9.50	2.18	11.7	11.5	2.00	1.44	17.0	0.52	0.18
TF17	CT3/ CT6	8.41	2.26	84.6	11.3	1.37	12.5	19.2	1.38	1.14	29.4	0.65	1.73
TF18	CT3/ CT6	6.44	2.12	84.6	10.0	2.12	13.0	16.0	1.12	1.19	30.9	0.70	1.13

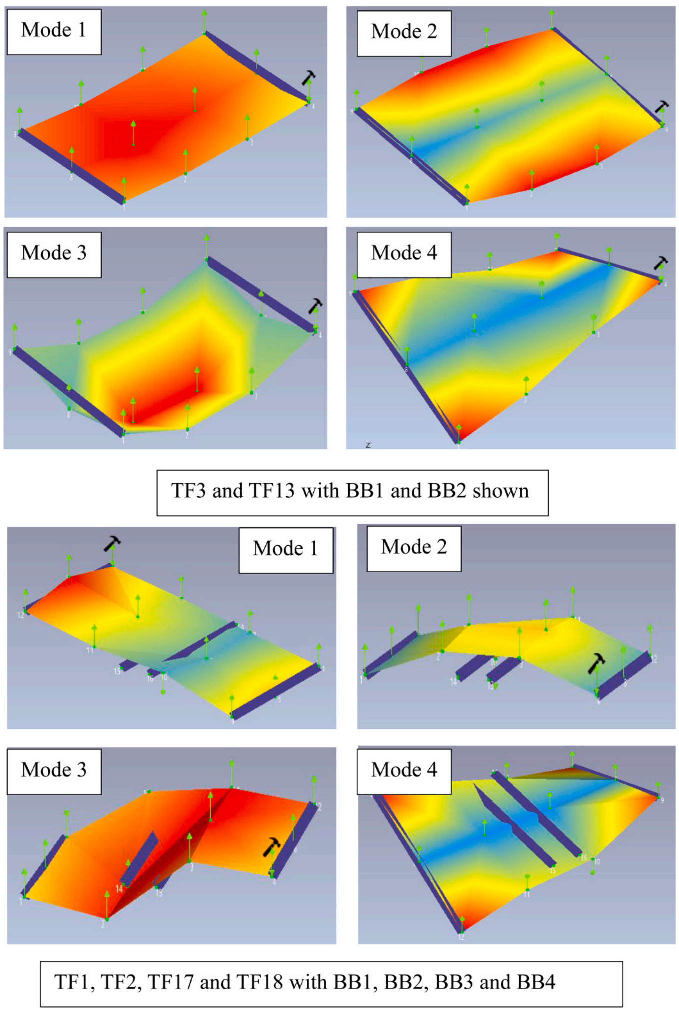

Fig. 6. Mode shapes of the floor systems with BBs shown with line elements. Floor configurations are defined in Table 2 and modal properties are given in Table 4.

demonstrates a consistent increase in natural frequency with increasing panel thickness. This is consistent for equivalent span arrangements, with CL5 floors exhibiting higher fundamental frequencies, reflecting the increased bending stiffness associated with the larger panel depth. This behaviour is consistent with classical plate bending theory, where flexural rigidity scales with the cube of thickness. The modal mass contribution (MMC) values reported in Table 4 indicate that the first mode consistently captures the dominant portion of the dynamic response, typically exceeding 70–90% of the total modal mass. The variation in MMC appears somewhat related to TFs with centre BBs in place, where these TFs appear to have higher MMC values compared to TFs with only outer BBs which report slightly lower MMC values.

Fig. 7 illustrates the influence of BB span (L_B) on the modal properties of the CL5 floor configurations. A clear inverse relationship between L_B and the natural frequency is observed for all four identified modes, with increasing L_B resulting in reduced modal frequencies. This behaviour is consistent with classical flexural theory, where increased span reduces global stiffness and increases structural flexibility. The effect is most pronounced for the fundamental (first) mode, which governs the dominant vibration response. In contrast, the damping ratios exhibit no consistent trend with span, suggesting damping is more sensitive to connection behaviour and material interaction than to global geometry alone. Fig. 8 isolates the influence of CLT clear span (L_F) while maintaining constant BB spans (L_B). Compared to the variation in L_B (Fig. 7), changes in L_F produce a more moderate yet systematic shift in modal behaviour. Increasing the CLT span from 6.6 m to 7.8 m leads to a consistent downward shift in the natural frequencies across all modes, reflecting the increased flexibility of the CLT panels between BBs. The reduction is evident in both the fundamental and higher modes, indicating that L_F contributes directly to the global bending stiffness of the composite floor system. The damping ratios however show scattered behaviour with no clear dependency on L_F. This suggests that energy dissipation mechanisms are governed more by connection interfaces and material interaction than by L_F. These results indicate that while L_F influences the absolute stiffness and modal frequencies of the floor, its effect is secondary to that of the BB span in governing overall dynamic behaviour.

Fig. 9 compares the modal properties of TFs with identical geometric configurations but different CLT thicknesses. For both TF1–TF17 and TF2–TF18 pairs, the CL5 panels consistently exhibit higher natural frequencies across all four identified modes. The increase is most pronounced for the fundamental mode, reflecting the strong dependence of bending stiffness on panel thickness.

3.2. *Influence of span and CLT thickness on vibration response*

Fig. 10 presents the variation of VDV and $a_{w,rms}$ with walking frequency for different L_B and CLT thicknesses (CL5 and CL3) with all results represented in Table 5. For all configurations, both VDV and $a_{w,rms}$ increase with walking frequency. The influence of L_B is clearly evident: longer spans ($L_B = 8$–9 m) consistently produce higher vibration levels than shorter spans ($L_B = 5$–6 m). Similarly, reducing CLT thickness from CL5 to CL3 results in increased vibration response due to reduced flexural rigidity. The combined effect of increased span and reduced thickness leads to the highest vibration levels observed in the study.

For acceleration-based assessment, ISO 10137 [32] defines comfort criteria through a response factor ($a_{w,rms}$ / 0.005 m/s^2). Based on the results in Fig. 10, the measured $a_{w,rms}$ range from 0.03 to 0.07 m/s^2 or from 6 to 14. For reference a response factor of 12 is a class 3 floor according to [24]. ISO 10137 [32] recommends response factors lower than 4 ($a_{w,rms}$ of 0.02 m/s^2) and 8 ($a_{w,rms}$ of 0.04 m/s^2) for residential (16 h day) and commercial floors (8 h day), respectively. However, it should be noted that an amplifying factor is introduced in ISO 10137 [32] to account for the number of events in a 16 h day (for residential applications). The measured VDV values range between 0.045 and 0.105 m·s$^{-1.75}$. For residential buildings, daytime reference bands are generally defined as 0.2–0.4 m·s$^{-1.75}$ (low probability of adverse comment), 0.4–0.8 m·s$^{-1.75}$ (adverse comments possible), and 0.8–1.6 m·s$^{-1.75}$ (adverse comments probable). All measured VDVs fall well below the lowest daytime threshold band, indicating a low probability of adverse comment according to ISO guidance. Similar trends are shown through Wang et al. [33] where increasing walking speed consistently leads to increases in both $a_{w,rms}$ and VDV responses. Further, Wang et al. [33] found that increases to the test floor aspect ratio (increases in thickness and/ or clear span) can influence also influence the $a_{w,rms}$ and VDV values as shown through this section of the study.

To isolate the influence of L_B on vibration response while maintaining constant CLT thickness and CLT span, the CL5 floors with $L_{F1} = 7.8$ m (TF3–TF7) were compared against those with $L_{F1} = 6.6$ m (TF8–TF12). The results in Table 5 show a consistent increase in both VDV and $a_{w,rms}$ with increasing L_B for both L_F cases. For example, in the $L_{F1} = 7.8$ m series (TF3–TF7), increasing L_B from 5 m to 9 m produces a clear amplification in vibration response across all walking frequencies. A similar trend is observed for the $L_{F1} = 6.6$ m series (TF8–TF12), confirming that L_B is a dominant parameter governing floor vibration performance. Although the absolute vibration levels are slightly higher for $L_{F1} = 7.8$ m, the sensitivity to L_B remains consistent between the two groups. This indicates that increasing L_B reduces the global stiffness of the system irrespective of CLT span, leading to increased dynamic amplification under walking excitation.

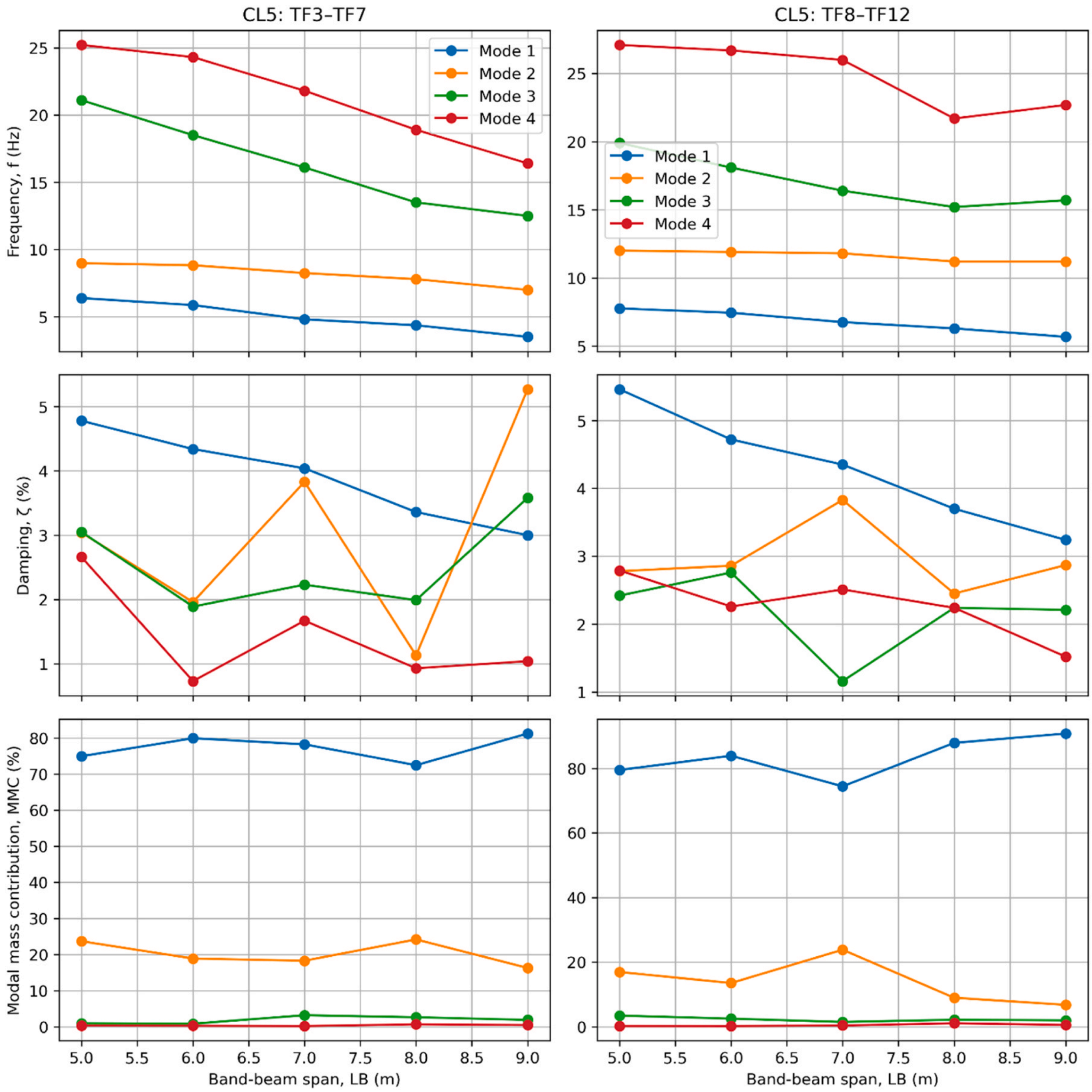

Fig. 7. Effect of the band-beam span on the modal properties of the floors with CL5 slabs.

The measured $a_{w,rms}$ values for both L_F groups correspond to response factors ranging between 6 and 14 as L_B increases. While longer spans push the response factor toward the upper end of this range, all values remain within multiplying factors commonly accepted for residential or office environments under intermittent instances of vibration. Similarly, the VDV values for both $L_{F1} = 7.8$ m and $L_{F1} = 6.6$ m configurations remain below the 0.2 $m \cdot s^{-1.75}$ daytime threshold associated with a low probability of adverse comment. Therefore, while increasing L_B systematically increases vibration magnitude, all CL5 configurations satisfy ISO comfort criteria within the investigated span range [32].

3.3. Influence of fixities on modal properties

Fig. 11a presents the variation in Mode 1 and Mode 2 frequencies and damping ratios for TF17 as the connection density between the CLT panels and BBs is increased from CT1 to CT6. The number of screws increases progressively from 144 (CT1) to 582 (CT6), representing increasing composite engagement between the slab and supporting band-beams. An increase in connection density produces a gradual increase in natural frequency for both modes. Mode 1 frequency increases from approximately 5.3 Hz at CT1 to approximately 6.0 Hz at CT6, representing a noticeable stiffening effect due to enhanced composite action. Mode 2 exhibits a smaller but consistent increase, rising from approximately 10.0 Hz to approximately 10.4 Hz. As noted in [24], the higher the stiffness of the shear connection the closer the effective flexural stiffness will be to that of a fully composite section.

Mode 1 damping decreases steadily as the number of screws increases, reducing from approximately 3.9% at CT1 to approximately 2.9% at CT6. The observed reduction in damping with increasing screw density is consistent with a transition from partial interaction to a more composite structural response [34]. At lower connection densities, relative slip at the CLT–BB interface and within the fastener group can be contributed to additional energy dissipation through micro-slip and local deformation mechanisms. As the number of screws increases, interfacial slip is progressively restrained. This reduction in relative movement limits frictional and connection-related energy dissipation, resulting in lower measured modal damping ratios despite the increase in global stiffness [34,35]. The configurations in Fig. 11b primarily differ in the orientation of the screws while maintaining comparable levels of connection engagement. The results for CT1 to CT6 (Fig. 11a) do not contain the Aladin resilient soundproofing material. Comparing cases with (CT7) and without (CT6) the Aladin, the natural frequency

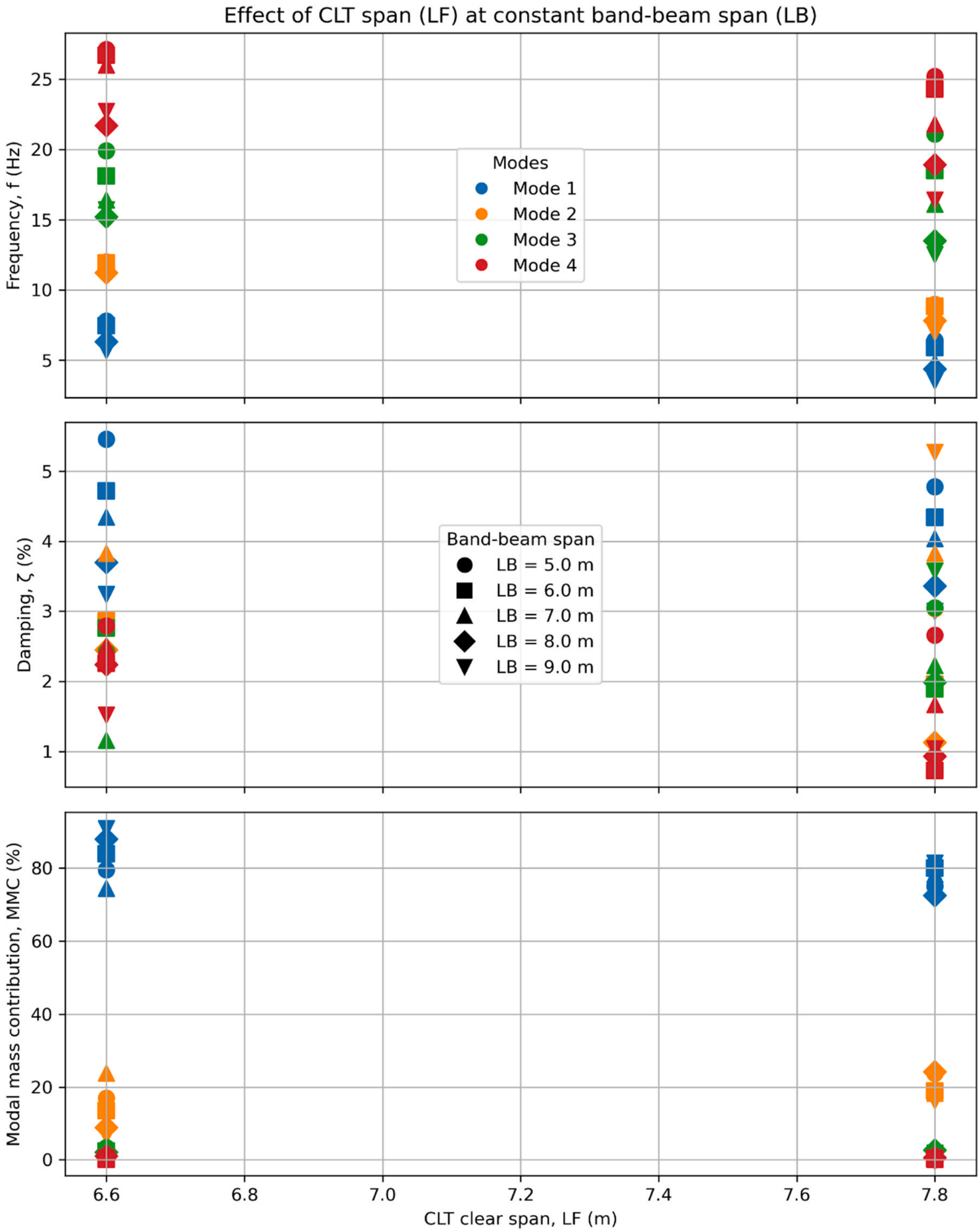

Fig. 8. Effect of CLT span on the modal properties of the floors with CL5 slabs, floors TF3–TF7 (LF = 7.8 m) are compared with TF8–TF12 (LF = 6.6 m) for corresponding band-beam spans (LB = 5–9 m).

does not appear to vary however damping increases by close to 1–3.87% for CT7 compared to CT6. This could be considered a notable increase as explored by [28,33,35,36] where a change in damping of 1% and greater is most likely to produce perceived changes in the floor performance for occupants.

For both TF17 and TF1, Mode 1 and Mode 2 frequencies vary within a narrow range across CT7–CT12 (Fig. 11b). This indicates that screw inclination has a secondary influence on global stiffness compared with connection density. While minor increases in frequency are observed for certain configurations, the overall magnitude of change remains limited.

In contrast, damping ratios exhibit greater variability with inclination. For TF17, noticeable changes in damping are observed between configurations, particularly in Mode 2 and Mode 3. However, the trends are not strictly monotonic, indicating that the damping response is governed by a combination of factors including fastener engagement, local deformation compatibility, and interaction between slab and band-beam components. For both TF17 and TF1, Mode 1 consistently carries the largest proportion of MMC, with higher modes contributing progressively less. Changes in inclination slightly redistribute MMC between Modes 2 and 3, but without altering the overall modal hierarchy. This

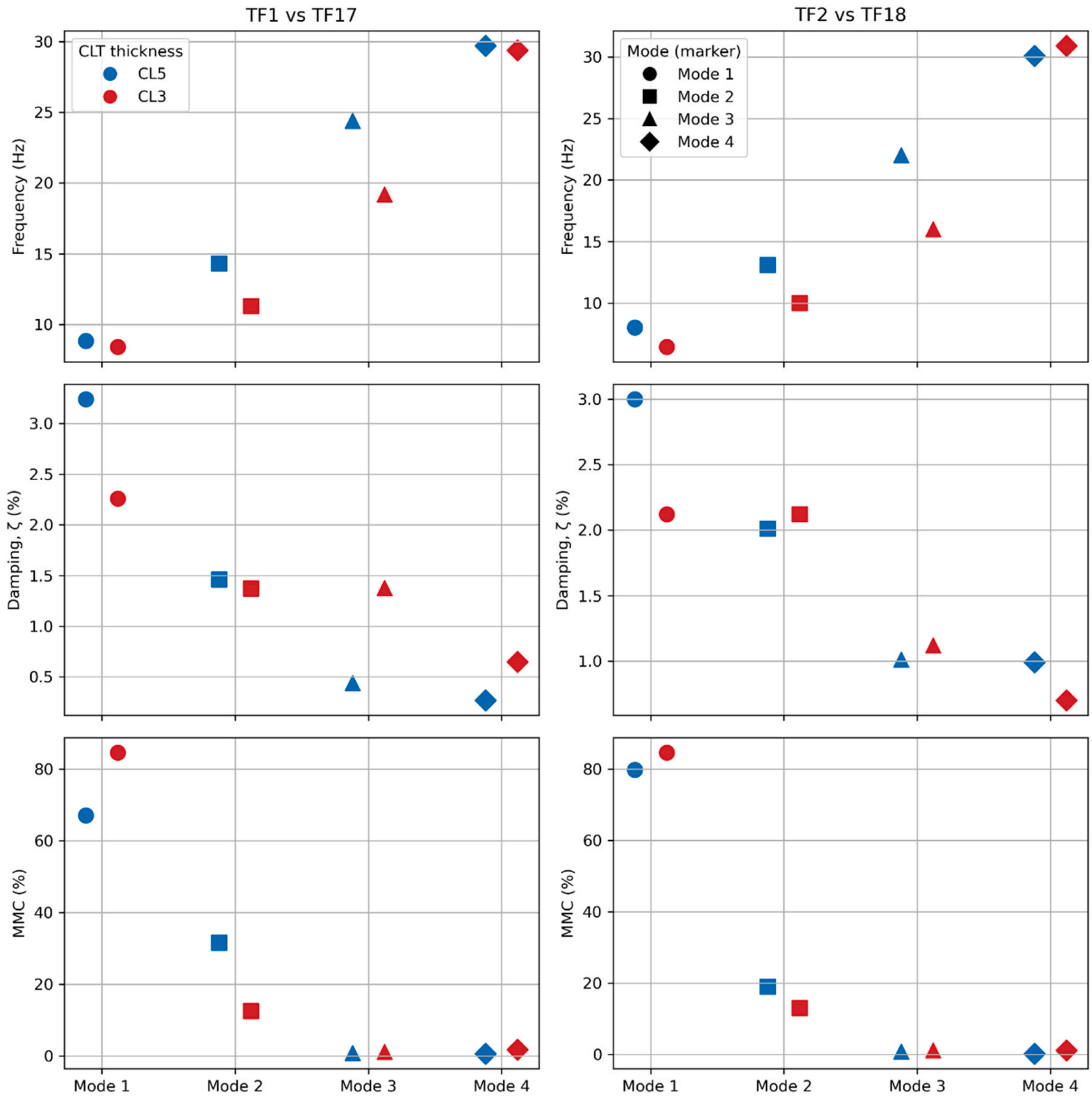

Fig. 9. Influence of CLT thickness on the modal properties of floor systems with four band beams.

indicates that while screw inclination can influence local dynamic behaviour, it does not fundamentally alter the global mode shape characteristics of the system.

3.4. Influence of fixities on vibration response

The influence of connection detailing on walking-induced vibration response is summarised in Table 6, with key trends illustrated in Fig. 12. It should be noted that the present investigation focused on the influence of practical connection layouts on the global dynamic behaviour of the floor system. Although the fastener arrangements were representative of typical construction practice, the study was not intended as a connection strength or shear-capacity design investigation. The measured responses nevertheless demonstrated effective composite interaction and load transfer between the CLT panels and band-beams.

The results present the variation in VDV and $a_{w,rms}$ with walking frequency for the different connection configurations. For TF17 (CL3, L_B = 9 m), connection density (CT1–CT6) and inclination configurations (CT7–CT9) significantly influence vibration magnitude. Increasing connection density generally reduces both VDV and $a_{w,rms}$, particularly at the higher walking frequencies (1.8–2.1 Hz). The reduction is most evident when comparing CT1 with the denser configurations (CT4–CT6). Inclination configurations (CT8 and CT9) exhibit comparatively lower VDV values than the lower-density configurations. With the Aladin resilient soundproofing material (CT7), there appears to be minor decrease in some VDV and $a_{w,rms}$ values when compared to the condition without Aladin (CT6). CT7 shows a reduction in $a_{w,rms}$ for 1.6 Hz as shown in Fig. 12 compared with CT6 which shows relatively consistent increases in $a_{w,rms}$ with increases in walking rates.

For TF1 (CL5, L_B = 9 m), a similar but less pronounced trend is observed. While differences between CT10–CT12 are smaller than those observed for TF17, connection configuration still affects both VDV and $a_{w,rms}$. The thicker CL5 slab inherently provides greater flexural stiffness, which moderates the sensitivity of vibration response to connection detailing. The measured $a_{w,rms}$ values across all configurations range approximately between 0.03 and 0.18 m/s^2 or response factor values ranging from 6 to 36. The highest response factors occur for TF17 with the lowest connection density (CT1) at lower walking frequencies. However, as connection density increases, response factors reduce and remain within multiplying factors commonly accepted for residential and office occupancies subjected to intermittent vibration. Across all configurations and walking frequencies, VDV values remain below

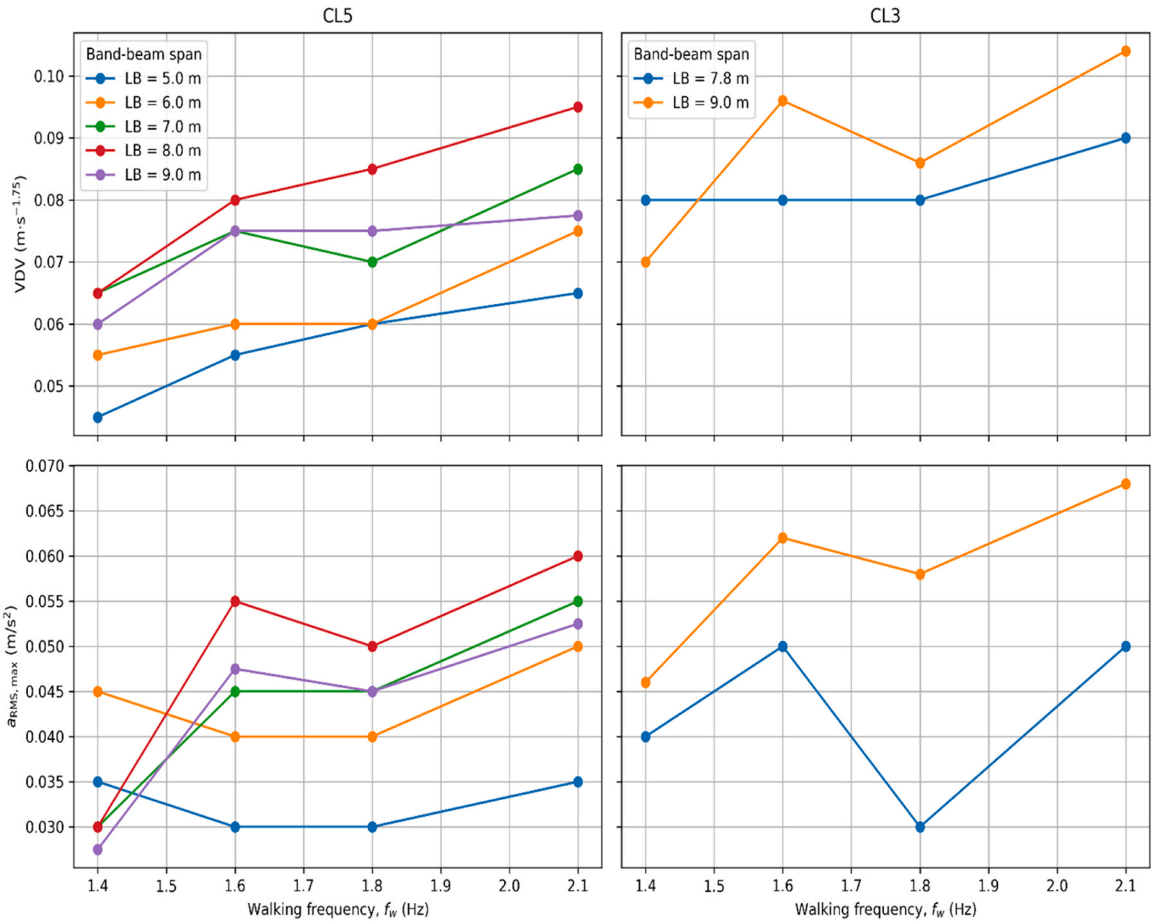

Fig. 10. Influence of band-beam span (L_B) and CLT thickness (CL5:TF3-TF7 and CL3:TF13-TF15) on vibration dose value and maximum acceleration under different walking frequencies.

Table 5
Vibration response of tested floors showing effect of CLT thickness and span lengths at different walking frequencies.

Test Floor	Connection Type	1.4 Hz			1.6 Hz			1.8 Hz			2.1 Hz		
		VDV m/s$^{1.75}$	a_{RMS} (m/s^2)		VDV m/s$^{1.75}$	a_{RMS} (m/s^2)		VDV m/s$^{1.75}$	a_{RMS} (m/s^2)		VDV m/s$^{1.75}$	a_{RMS} (m/s^2)	
			mean	max		mean	max		mean	max		mean	max
TF1	CT9/ CT6	0.038	0.012	0.020	0.055	0.017	0.036	0.053	0.015	0.032	0.064	0.015	0.046
TF2	CT9/ CT6	0.032	0.009	0.019	0.042	0.011	0.027	0.058	0.016	0.035	0.041	0.010	0.025
TF3	CT9/ CT6	0.080	0.024	0.057	0.104	0.034	0.065	0.113	0.036	0.065	0.118	0.038	0.068
TF4	CT9/ CT6	0.072	0.024	0.043	0.080	0.022	0.055	0.096	0.034	0.054	0.104	0.030	0.061
TF5	CT9/ CT6	0.068	0.022	0.040	0.073	0.022	0.039	0.079	0.022	0.051	0.086	0.025	0.056
TF6	CT9/ CT6	0.057	0.018	0.034	0.061	0.018	0.039	0.065	0.021	0.037	0.074	0.022	0.045
TF7	CT9/ CT6	0.049	0.016	0.026	0.055	0.017	0.030	0.062	0.020	0.032	0.070	0.021	0.043
TF8	CT9/ CT6	0.089	0.030	0.055	0.105	0.029	0.063	0.077	0.022	0.050	0.095	0.028	0.073
TF9	CT9/ CT6	0.058	0.020	0.036	0.082	0.026	0.052	0.070	0.020	0.047	0.090	0.025	0.063
TF10	CT9/ CT6	0.057	0.017	0.034	0.077	0.021	0.046	0.062	0.019	0.041	0.084	0.025	0.051
TF11	CT9/ CT6	0.052	0.014	0.031	0.062	0.017	0.040	0.061	0.017	0.040	0.083	0.025	0.050
TF12	CT9/ CT6	0.044	0.013	0.027	0.051	0.017	0.033	0.059	0.017	0.033	0.059	0.017	0.033
TF13	CT3/ CT6	0.032	0.021	0.029	0.082	0.019	0.058	0.055	0.020	0.059	0.080	0.018	0.061
TF14	CT3/ CT6	0.081	0.030	0.037	0.081	0.033	0.052	0.083	0.033	0.031	0.091	0.016	0.047
TF15	CT3/ CT6	0.106	0.025	0.063	0.129	0.032	0.078	0.140	0.034	0.086	0.148	0.033	0.085
TF16	CT3/ CT6	0.088	0.017	0.055	0.123	0.028	0.073	0.113	0.036	0.065	0.118	0.038	0.068
TF17	CT3/ CT6	0.038	0.012	0.020	0.055	0.017	0.036	0.053	0.015	0.032	0.064	0.015	0.046
TF18	CT3/ CT6	0.080	0.024	0.057	0.104	0.034	0.065	0.072	0.017	0.039	0.113	0.024	0.068

0.22 $m \cdot s^{-1.75}$. These values are within the lower daytime band (0.2–0.4 $m \cdot s^{-1.75}$) associated with a low probability of adverse comment in residential buildings.

3.5. Influence of superimposed load on modal properties

The influence of superimposed dead load (SDL) on the modal characteristics of the floor systems is summarised in Table 7, with representative mode shapes shown in Fig. 13. For both TF17 (CL3) and TF1 (CL5), the introduction of the 30 kg/m^2 SDL produces measurable

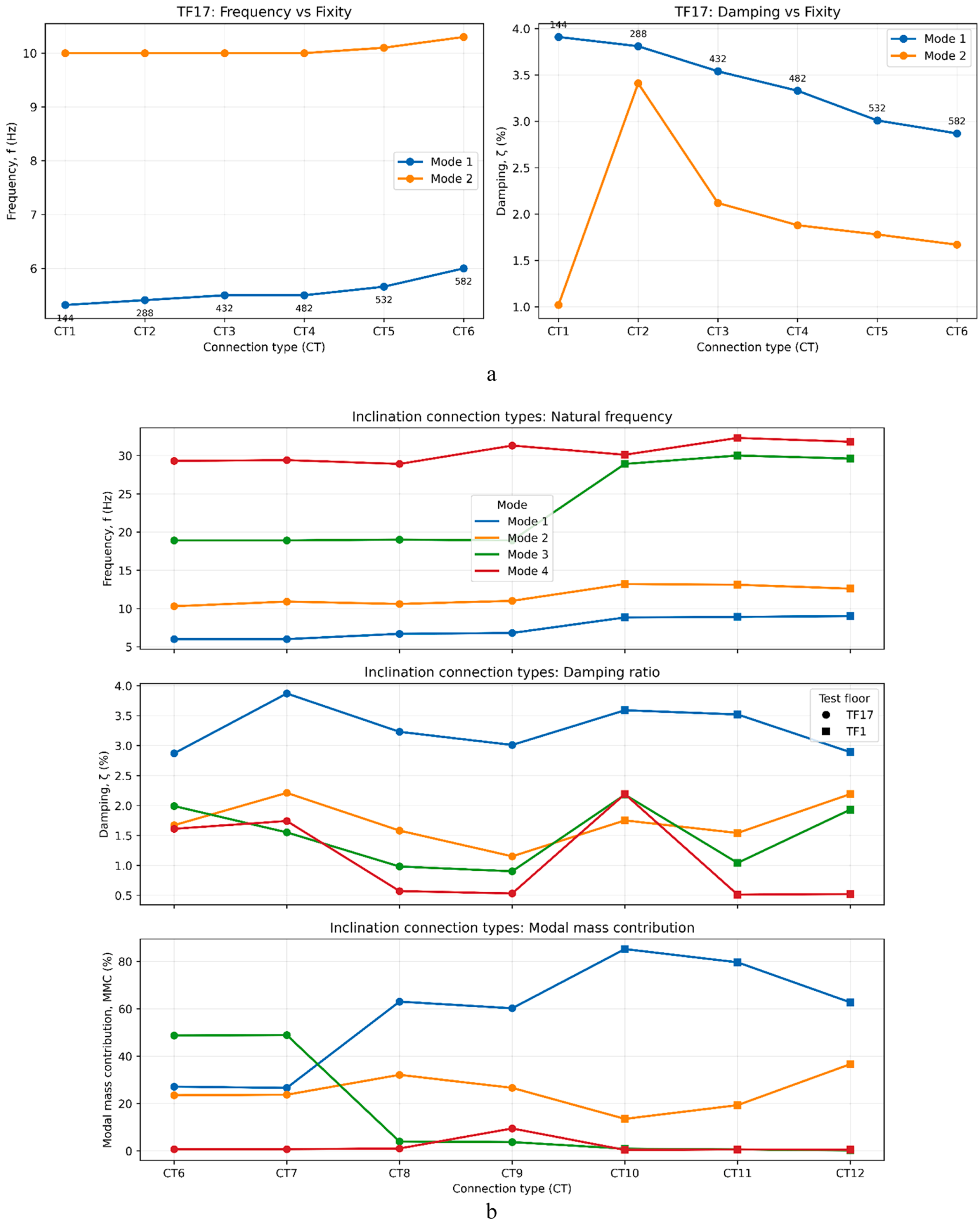

Fig. 11. (a) Influence of connection density (CT1–CT6) on the modal properties of TF17 (CL3, $L_B = 9$ m), and (b) effect of screw inclination connection types (CT7–CT11) on the modal properties of TF17 and TF1 floors.

changes in modal properties. A modest reduction in natural frequencies is observed for the fundamental mode of TF17 (8.28 Hz to 8.41 Hz), while Mode 2 frequency increases slightly (10.90 Hz to 11.30 Hz). For TF1, the fundamental frequency increases marginally from 8.08 Hz to 8.23 Hz, while Mode 2 increases from 13.90 Hz to 14.30 Hz. These variations remain relatively small, indicating that the additional 30 kg/m^2 load does not significantly alter global stiffness but influences dynamic behaviour through mass redistribution and mode coupling.

Table 6
Vibration response of tested floors showing effect of fixities at different walking frequencies.

Test Floor	Connection Type	1.4 Hz			1.6 Hz			1.8 Hz			2.1 Hz		
		VDV m/s1.75	*aRMS* (m/s2)		VDV m/s1.75	*aRMS* (m/s2)		VDV m/s1.75	*aRMS* (m/s2)		VDV m/s1.75	*aRMS* (m/s2)	
			mean	max		mean	max		mean	max		mean	max
TF17	CT1	0.143	0.061	0.177	0.201	0.067	0.111	0.210	0.055	0.122	0.217	0.074	0.121
TF17	CT2	0.138	0.057	0.166	0.180	0.050	0.070	0.150	0.036	0.100	0.192	0.044	0.064
TF17	CT3	0.098	0.034	0.060	0.117	0.033	0.036	0.115	0.031	0.064	0.131	0.032	0.048
TF17	CT4	0.105	0.030	0.055	0.123	0.034	0.043	0.121	0.034	0.066	0.134	0.030	0.040
TF17	CT5	0.084	0.028	0.045	0.105	0.029	0.046	0.118	0.028	0.060	0.103	0.026	0.036
TF17	CT6	0.100	0.031	0.038	0.105	0.033	0.049	0.120	0.038	0.061	0.098	0.029	0.040
TF17	CT7	0.085	0.024	0.038	0.092	0.032	0.029	0.116	0.025	0.048	0.095	0.026	0.036
TF17	CT8	0.078	0.022	0.051	0.086	0.027	0.057	0.104	0.033	0.066	0.088	0.027	0.042
TF17	CT9	0.065	0.021	0.044	0.082	0.041	0.053	0.103	0.030	0.064	0.062	0.025	0.045
TF1	CT10	0.080	0.023	0.033	0.106	0.032	0.047	0.098	0.035	0.071	0.089	0.042	0.039
TF1	CT11	0.068	0.022	0.038	0.092	0.024	0.068	0.105	0.026	0.055	0.066	0.033	0.041
TF1	CT12	0.059	0.017	0.023	0.080	0.022	0.047	0.088	0.024	0.045	0.065	0.028	0.035

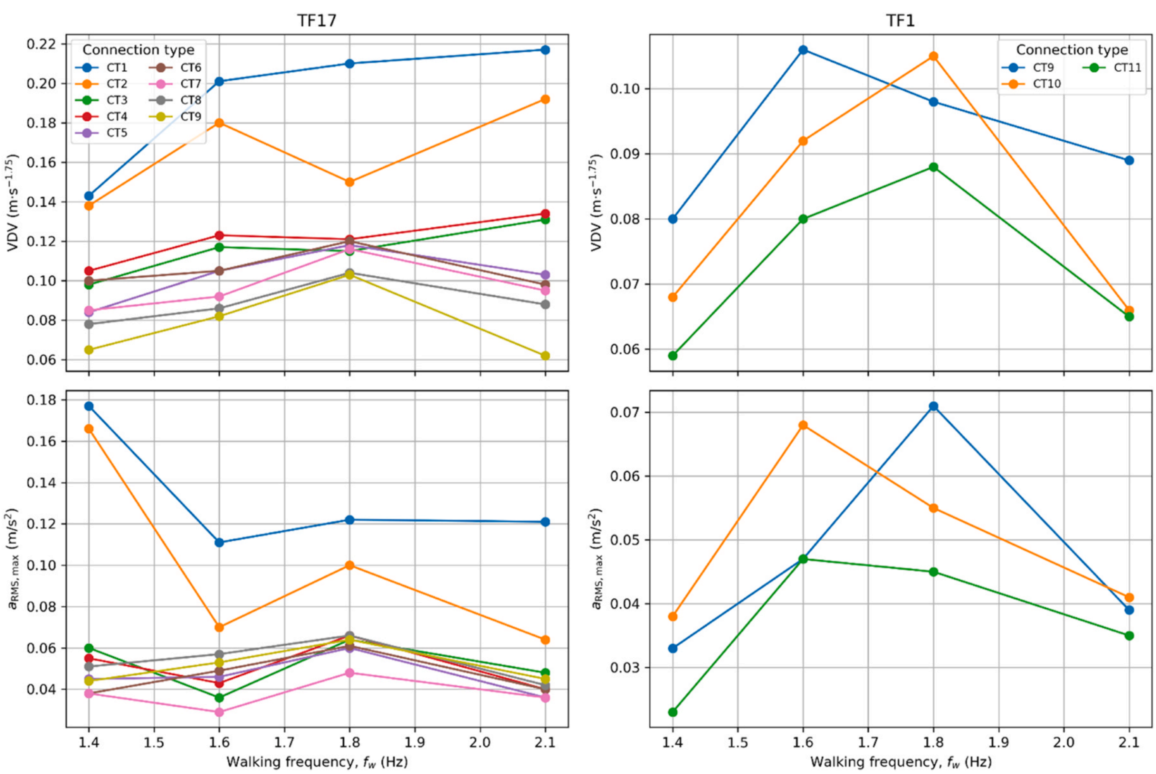

Fig. 12. The effect of connection detailing on walking-induced vibration response.

Table 7
Experimental modal properties of floors TF1 and TF17 with and without the superimposed SDL of 30 kg/m^2. Mode shapes are shown in Fig. 13.

Test Floor	CLT	Connection Type	SDL	Mode 1			Mode 2		
			(kg/m^2)	*f* (Hz)	ζ (%)	MMC (%)	*f* (Hz)	ζ (%)	MMC (%)
TF17	CL3	CT6	–	8.28	3.13	26.7	10.90	1.57	73.05
TF17	CL3	CT6	30	8.41	2.95	96.3	11.30	1.37	2.98
TF1	CL5	CT9	–	8.08	3.18	17.9	13.90	1.98	81.80
TF1	CL5	CT9	30	8.23	1.86	80.30	14.30	1.46	18.90

For TF17 under zero SDL, Mode 2 dominates the vertical response with 73.05% MMC, while Mode 1 contributes only 26.7%. After application of the 30 kg/m^2 load, this distribution reverses: Mode 1 becomes dominant with 96.3% MMC, and Mode 2 reduces to 2.98%. A similar mode shift is observed for TF1where zero SDL returns a 81.8% MMC for Mode 2, whereas with 30 kg/m^2 SDL, Mode 1 becomes dominant with 80.30% MMC. This shift in modal dominance indicates a reordering of the effective vibration modes under asymmetric loading. The additional mass applied to one side of the floor modifies the inertia distribution and reduces structural symmetry, thereby altering modal coupling and participation factors. As a result, the mode that previously contributed most to the vertical response is superseded by another mode once the load is introduced. Fig. 13 further illustrates that the introduction of SDL leads to visibly unsymmetric mode shapes.

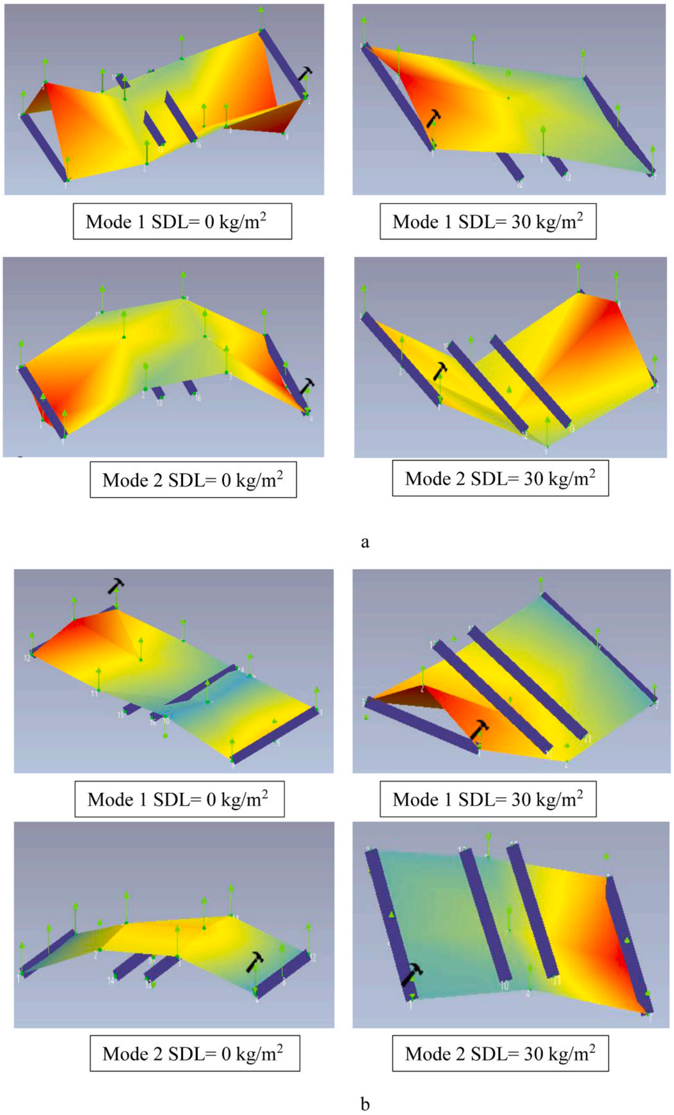

Fig. 13. Mode shapes with BBs with large vertical modal mass contribution of (a) TF17 (CL3) and (b) TF1 (CL5), showing effect of unsymmetric superimposed loading of 30 kg/m^2. Modal properties are given in Table 7.

3.6. Influence of superimposed load on vibration response

The effect of an asymmetric SDL of 30 kg/m^2 on vibration response is illustrated in Fig. 14 for CL5–TF1 and CL3–TF17 floors. The comparison is made under walking excitation frequencies ranging from 1.4 to 2.1 Hz. For CL5–TF1, the introduction of 30 kg/m^2 generally reduces the VDV across the investigated walking frequencies. The reduction is most noticeable at lower frequencies (1.4–1.6 Hz), where the unloaded configuration produces the highest response. At higher walking frequencies (1.8–2.1 Hz), the difference between loaded and unloaded states becomes smaller, indicating that the added mass slightly shifts the dynamic characteristics but does not significantly amplify the response. At lower walking frequencies (1.4–1.6 Hz), CL3-TF17 VDV increases with the use of an SDL compared to the unloaded case, suggesting that the added mass shifts the dynamic characteristics closer to the excitation range. At 1.8 Hz, the loaded configuration shows the highest response for this floor, indicating a possible proximity to modal interaction following the modal redistribution observed in Section 3.5. At 2.1 Hz, however, the loaded case produces a slightly lower VDV than the unloaded configuration.

When assessed against ISO 10137 [32] and BS 6472–1 [37] VDV

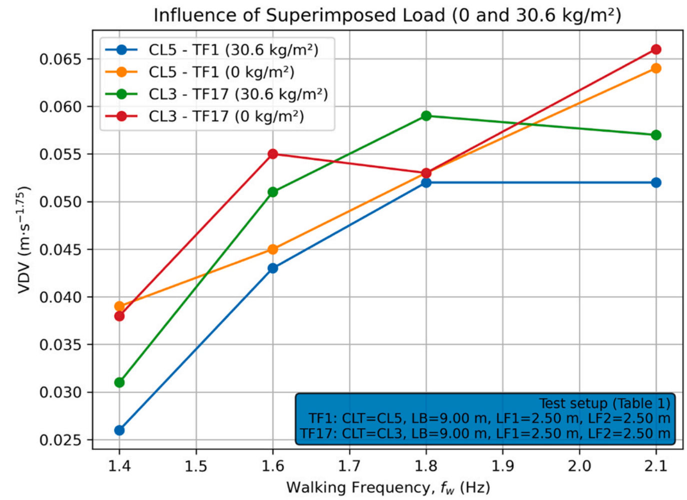

Fig. 14. Influence of superimposed dead load (SDL) of 0 and 30 kg/m^2 on vibration dose value (VDV).

criteria for residential buildings, all measured VDVs remain well below the daytime acceptability bands (0.2–0.4 m/s $^{1.75}$ for low probability of adverse comments). The maximum recorded values in Fig. 14 are approximately 0.065 m/s $^{1.75}$, which are significantly lower than the threshold for adverse comments. Therefore, from a serviceability perspective, both floor systems satisfy international vibration acceptability criteria under the investigated loading and excitation conditions.

4. Conclusions

This study experimentally investigated the dynamic behaviour and vibration serviceability of long-span CLT BB floor systems using a full-scale modular laboratory setup (up to 9 m × 9 m). A comprehensive parametric program was conducted using both EMA and controlled walking tests to quantify the influence of BB span (L_B), CLT span (L_F), CLT thickness (CL3 and CL5), connection density and inclination, and an asymmetric SDL (30 kg/m^2). Among the investigated parameters, reducing band-beam span and using thicker CLT panels were found to be the most effective means of improving vibration serviceability, while the addition of resilient material provided a significant increase in damping. Small differences in damping ratio should be interpreted with caution; however, the approximately 30–35% increase in Mode 1 damping associated with the resilient layer is substantially larger than the observed variation between impact and heel-drop estimates and is therefore considered a meaningful trend. Increasing connection density beyond moderate levels yielded diminishing benefits, and screw inclination had only a minor effect.

Key findings are summarised below:

- Increasing L_B consistently reduced natural frequencies and increased walking-induced response (VDV and $a_{w,rms}$), confirming L_B as the dominant design parameter controlling serviceability for BB-supported CLT floors. Increasing L_F reduced natural frequencies across all identified modes, but its influence on damping was scattered and generally weaker than the effect of L_B. Increased CLT thickness improves vibration performance. For comparable layouts, the thicker CL5 slabs produced higher natural frequencies and reduced walking-induced response compared with CL3, consistent with increased flexural rigidity.
- Increasing screw numbers (CT1 to CT6) was found to increase Mode 1 and 2 frequencies, indicating improved composite interaction. Measured damping decreased with increasing connection density, consistent with a more fully engaged system with reduced interfacial slip and reduced frictional/ micro-slip energy dissipation

mechanisms. Across the inclination configurations (CT7 to CT12), frequency changes were relatively small compared to density effects, while damping showed greater variability, indicating sensitivity to local interaction and deformation compatibility at the connection interface.

- The asymmetric 30 kg/m^2 SDL produced a clear shift in modal mass dominance, with Mode 1 becoming the primary vertical response mode once the load was applied. The corresponding mode shapes became visibly unsymmetric due to eccentric mass distribution in the four-BB configurations.
- Inclusion of the Aladin resilient soundproofing material increased Mode 1 damping by approximately 1% in absolute terms without materially changing natural frequencies. This enhanced interfacial energy dissipation produced modest reductions in walking-induced $a_{w,rms}$ and VDV thereby improving vibration serviceability performance without compromising structural behaviour.
- VDVs measured across the span, thickness, connection, and loading cases remained well below the ISO/BS daytime residential VDV threshold band associated with low probability of adverse comment (0.2–0.4 $m\cdot s^{-1.75}$). Response factors increased with span and reduced thickness but remained within ranges commonly adopted for intermittent vibration assessment, noting ISO 10137 [32] event-frequency adjustment considerations.

Additional research is recommended to link these measured performance characteristics with perception results from user observations. Furthermore, linking the laboratory measurements with those from potential in-situ field experiments would determine alignment and accuracy of setup.

CRediT authorship contribution statement

Adam Faircloth: Writing – original draft, Validation, Software, Methodology, Investigation, Formal analysis, Data curation, Conceptualization. **Benoit P. Gilbert:** Writing – review & editing, Validation, Supervision, Resources, Methodology. **Hassan Karampour:** Writing – review & editing, Supervision, Resources, Project administration, Funding acquisition, Formal analysis, Conceptualization. **Ian Underhill:** Writing – review & editing, Visualization, Software, Resources, Methodology. **Chandan Kumar:** Writing – review & editing, Validation, Resources, Methodology, Formal analysis, Conceptualization.

Declaration of Competing Interest

The authors declare that they have no known competing financial interests or personal relationships that could have appeared to influence the work reported in this paper.

Acknowledgements

The authors would like to acknowledge the financial support provided by the Australian Research Council funded Advanced Timber Hub (IH220100016) as well as financial, technical, and equipment support provided by Griffith Universities School of Engineering and Built Environment, and the Queensland Department of Primary Industries' Salisbury Research Facility. For materials provided to the research team such as CLT, BBs, fasteners and resilient materials, project partners such as XLam (namely Mr Tom Watts) and Rothoblaas (namely Mr Sebastian Jaimes) are acknowledged. Further specific acknowledgements are made to Dr Huaizhong Li and Mr Farshad Janghorban for their support and advice provided throughout the studies' experimental process.

References

[1] Kremer P, Symmons M. Perceived Barriers to the Widespread Adoption of Mass Timber Construction: An Australian Construction Industry Case Study. Mass Timber Constr J 2018;1:1–8.
[2] McGavin RL, Dakin T, Shanks J. Mass-timber Construction in Australia: Is CLT the only Answer? Bioresources 2020;15(3):4642–5. https://doi.org/10.15376/biores.15.3.4642-4645.
[3] Evison CD, Kremer P, Guiver J. Mass Timber Construction in Australia & New Zealand – Status, and Economic and Environmental Influences on Adoption. Wood Fibre Sci 2018;50:128–38.
[4] Firoozi AA, Firoozi AA, Oyejobi DO, Avudaiappan S, Flores ES. Emerging trends in sustainable building materials: Technological innovations, enhanced performance, and future directions. Results Eng 2024;24:103521. https://doi.org/10.1016/j.rineng.2024.103521.
[5] Brandner R, Flatscher G, Ringhofer A, Schickhofer G, Thiel A. Cross Laminated Timber (CLT): Overview and Development. Eur J Wood Wood Prod 2016;74:331–51. https://doi.org/10.1007/s00107-015-0999-5.
[6] Middleton R. Timber Construction using CLT. 21/02/2017 Reid Middlet Civil Struct Eng 2017. https://www.reidmiddleton.com/reidourblog/timber-construction-using-clt. 21/02/2017.
[7] Lehmann S, Kremer P. Filling the Knowledge Gaps in Mass Timber Construction: where are the Missing Pieces, what are the Research Needs? Mass Timber Constr J 2023;6.
[8] Vairo M, Silva VP, Icimoto FH. Behavior of cross-laminated timber panels during and after an ISO-fire: An experimental analysis. Results Eng 2023;17:100878. https://doi.org/10.1016/j.rineng.2023.100878.
[9] K. Lewis, B. Basaglia, R. Stirling, K. Crews, The use of Cross Laminated Timber for Long Span Flooring in Commercial Buildings, WCTE 2016 22-25 Aug Vienna, Austria (2026) 4813-4821.
[10] Basaglia B, Li J, Shrestha R, Crews K. Response Prediction to Walking-Induced Vibrations of a Long-Span Timber Floor. J Struct Eng 2021;147(2).
[11] Karampour H, Piran F, Faircloth A, Talebian N, Miller D. Vibration of Timber and Hybrid Floors: A Review of Methods of Measurement, Analysis and Design 2023;13(7):1756. https://doi.org/10.3390/buildings13071756.
[12] Sierra IEM, Salinas JC, Manzano MAR. A. P. G. Zuniga, Evaluation of human-induced vibration of ferrocement in lightweight constructive systems. Results Eng 2025;26:105376. https://doi.org/10.1016/j.rineng.2025.105376.
[13] Wang W, Liang S, Zhu X, Xu Y, Han T, Xie Z, et al. Research on the dynamic characteristics and serviceability of novel PSRC floor. Results Eng 2025;28:107505. https://doi.org/10.1016/j.rineng.2025.107505.
[14] J. Weckendorf, B. Zhang, A. Kermani, D. Reid, Damping Characteristics of Timber Flooring Systems with Respect to Low-Frequency Vibration Modes, WCTE 2008 2-5 Jun Miyazaki Japan (2008).
[15] Faircloth A, Karampour H, Gilbert BP, Watts T, Li H, Burdon N, et al. Design Uncertainty in Long Span Mass Timber Floors: Proposed Band-Beam Solution. WCTE 2025 22-26 Jun Brisb Aust 2025:466–72. https://doi.org/10.52202/080513-0058.
[16] C. Guo, R. Jackson, M. Shahnewaz, J. Zhou, Vibration Performance of a Beamless Cross Laminated Timber-Concrete Composite Slab Band Floor System for 10-Storey Limberlost Place, WCTE 2025 22-26 Jun Brisbane Australia (2025) 3272-3279, https://doi.org/10.52202/080513-0400.
[17] IStructE, Limberlost Place, George Brown College, https://www.istructe.org/structural-awards/projects/2025/limberlost-place/, accessed 07/02/2026.
[18] Timbers Hyne. Marybgh Fire Rescue Station 07/02/2026. https://www.hyne.com.au/article/maryborough-fire-and-rescue-station (accessed).
[19] Gleason TM. Evaluation of Structural Systems for Mass Timber Buildings in Low to Moderate Seismic Regions. Department of Civil and Environmental Engineering, Massachusetts Institute of Technology (MIT) Master's Thesis; 2019.
[20] L. Hu, Y.H. Chui, Canadian CLT Handbook: Cross Laminated Timber, Chapter 7 Vibration Performance of Cross-Laminated Timber Floors, FPInnovations, Ch 7 Point-Claire QC, Canada, SP-529E (2019).
[21] Faircloth A, Karampour H, Hamm P, Muller T, Pavic A, Reynolds P, et al. Global State of Knowledge on Human-Induced Sound and Vibration Events: Defining Future Research Directions for Mass Timber Products. J Wood Sci 2026;72(1). https://doi.org/10.1186/s10086-026-02254-z.
[22] XLam, XLam CLT Panel Product Datasheet, Sep 2023 (2023).
[23] Faircloth A, Brancheriau L, Karampour H, Kumar C. Evaluation of Full-Sized and Thick CLT Panels using in-line Non-Destructive Techniques. Wood Sci Mater Eng 2023;19(3):1–14. https://doi.org/10.1080/17480272.2023.2286622.
[24] Eurocode 5: Design of timber structures, Part 1-1: General – common rules and rules for buildings, EN 1995-1-1, Brussels Belgium, Vol. 1, No. 1, 2025.
[25] EN 16929, Test methods, Timber floors – Determination of vibration properties, Brussels Belgium, 2018.
[26] SVIBS, Modal estimation window – stochastic subspace identification, ARTeMIS Modal, retrieved 07/06/2026,https://www.svibs.com/resources/ARTeMIS_Modal_Help/SSI%20Modal%20Estimation%20window.html.
[27] Bajric A, Hogsberg J, Rudinger F. Evaluation of Damping Estimates by Automated Operational Modal Analysis for Offshore Wind Turbine Tower Vibrations. Renew Energy 2018;116(Part B):153–63. https://doi.org/10.1016/j.renene.2017.03.043.
[28] Labonnote N. Damping in Timber Structures. Trondheim Norway: Department of Structural Engineering Norwegian University of Science and Technology PhD Doctoral Thesis; 2012.
[29] SVIBS, Technical Specifications for ARTeMIS Modal 8.0, SVIBS A/S, Aalborg, Denmark, March 2025.

[30] M.R. Willford, P., Young, A Design Guide for Footfall Induced Vibration of Structures, MPA The Concrete Centre CCIP-016 (2007) ISBN: 1-904482-29-5.
[31] ISO 2631-1, Evaluation of Human Exposure to Whole-body Vibration, Part 1: General Requirements, Sydney Australia (2001).
[32] ISO 10137, Basis for Design of Structures, Serviceability of Buildings and Walkways Against Vibrations, Geneva Switzerland (2007).
[33] Wang C, Chang WS, Yan W, Huang H. Predicting the human-induced vibration of cross laminated timber floor under multi-person loadings. Structures 2021;29: 65–78. https://doi.org/10.1016/j.istruc.2020.10.074.
[34] J. Zhou, Y.H. Chui, L. Zhang, G. Li, Vibration Performance and Stiffness Properties of Mass Timber Panel-Concrete Composite Floors with Notched Connections, Journal of Structural Engineering 148 (9) https://10.1061/(ASCE)ST.1943-541X.0003450.
[35] Bresolin JM, Kripka M. Z. M. C. Pravia, Experimental study of human-induced vibrations on glued laminated timber floors. ISSN 2352-0124 Structures 2025;80: 110083. https://doi.org/10.1016/j.istruc.2025.110083.
[36] Hamm P, Knöpfle V, Ruf J, Bacher P, Gotz T. Full Scale Vibration Tests on a Long Span Timber Floor. WCTE 2023 19-22 Jun Oslo Nor 2023. https://doi.org/10.52202/069179-0245.
[37] BS 6472-1. Guide to Evaluation of Human Exposure to Vibration in Buildings. London UK: British Standards; 2008.